Published in final edited form as:
J Neuroimmune Pharmacol. 2013 September ; 8(4): 998–1009. doi:10.1007/s11481-013-9471-7.

Adenosine triphosphate released from HIV-infected macrophages regulates glutamatergic tone and dendritic spine density on neurons

Luis B. Tovar-y-Romo[1], **Dennis L. Kolson**[2], **Veera Venkata Ratnam Bandaru**[1], **Julia Drewes**[3], **David R. Graham**[3], and **Norman J. Haughey**[1,3]

[1]Department of Neurology, Richard T. Johnson Division of Neuroimmunology and Neurological Infections, Johns Hopkins University School of Medicine, Baltimore, MD.

[2]Department of Neurology, Perelman School of Medicine University of Pennsylvania, Philadelphia, PA.

[3]Department of Molecular and Comparative Pathobiology; Johns Hopkins University School of Medicine, Baltimore, MD.

Abstract

Despite wide spread use of combination antiretroviral therapy (cART) in developed countries, approximately half of HIV-infected patients will develop impairments in cognitive function. Accumulating evidence suggests that neuronal dysfunction can be precipitated by HIV-infection of macrophages by mechanisms that involve alterations in innate and adaptive immune responses. HIV-infection of macrophages is known to increase the release of soluble neurotoxins. However, the composition of products released from infected macrophages is complex and not fully known. In this study we provide evidence that ATP and other immuno-/neuromodulatory nucleotides are exported from HIV-infected macrophages and modify neuronal structure. Supernatants collected from HIV-infected macrophages (HIV/MDM) contained large amounts of ATP, ADP, AMP and small amounts of adenosine, in addition to glutamate. Dilutions of these supernatants that were sub-threshold for glutamate receptor activation evoked rapid calcium flux in neurons that were completely inhibited by the enzymatic degradation of ATP, or by blockade of calcium permeable purinergic receptors. Applications of these high-dilution HIV/MDM onto neuronal cultures increased the amount of extracellular glutamate by mechanisms dependent on purinergic receptor activation, and downregulated spine density on neurons by mechanisms dependent on purinergic and glutamate receptor activation. We conclude from these data that ATP released from HIV-infected macrophages downregulates dendritic spine density on neurons by a mechanism that involves purinergic receptor mediated modulation of glutamatergic tone. These data suggest that neuronal function may be depressed in HIV infected individuals by mechanisms that involve macrophage release of ATP that triggers secondary effects on glutamate handling.

Keywords

HIV; purinergic receptors; HIV-associated neurocognitive disorders; NMDA; glutamate; P2X; calcium; excitotoxicity; ATP; adenine nucleotides

Corresponding author: Norman J. Haughey, Department of Neurology, The Johns Hopkins University School of Medicine, Pathology 517, 600 North Wolfe Street, Baltimore, MD 21287, Phone: 443-287-3825, Fax: 410-955-0672.

COMPETING INTERESTS

The authors have no conflicts of interest or competing interests to disclose.

BACKGROUND

Despite the widespread use of combination anti-retroviral therapy (cART) in developed countries, nearly 40% of HIV-infected individuals will develop neurological impairments. These impairments range from asymptomatic neurocognitive impairment (ANI) that is discernable through neurocognitive testing, mild neurocognitive disorder (MND) with impairments in every day functions, to HIV-associated dementia (HAD) with severe limitations in the activities associated with every day living (Heaton et al., 2010; McArthur et al., 2010; Vivithanaporn et al., 2010; Heaton et al., 2011). Currently, ANI is the most common HIV-associated neurocognitive disorder (HAND) in cART treated individuals that is commonly associated with considerable brain pathology (Everall et al., 2009). Although HIV-infected subjects are living longer due to continued advancements in cART, the presence of HAND is associated with a shorter life expectancy (Vivithanaporn et al., 2010). Presumably, this shorter lifespan is the manifestation of fulminant CNS pathology. Although exact mechanisms for the continued occurrence HAND and reduced lifespan are not fully understood, they are thought to involve complex interactions of viral and host factors that are damaging to the CNS (Kraft-Terry et al., 2009; McArthur et al., 2010).

The infection of macrophages by HIV can have profound effects on brain function (Hult et al., 2008). Even in cART treated individuals, certain populations of HIV-infected macrophages transmigrate into the CNS and can be found in perivascular cuffs and in parenchyma (Langford et al., 2003; Gras and Kaul, 2010; Buckner et al., 2011). These infected monocytes have altered metabolic functions that increase the release of immunomodulatory factors and amino acids such as arachidonic acid and glutamate (Tian et al., 2012; Koenig et al., 1986; Dreyer and Lipton, 1995; Yadav and Collman, 2009; Yao et al., 2010; Thompson et al., 2011). The removal of viral and proteinaceous components from the media of HIV-infected macrophages (HIV/MDM) revealed that a low molecular weight compounds acting through glutamatergic receptors were toxic to neurons (O'Donnell et al., 2006; Erdmann et al., 2007; Erdmann et al., 2009). HIV/MDM media was found to contain concentrations of glutamate toxic to neurons by effects mediated through the hyperactivation of NMDA receptors (O'Donnell et al., 2006). In preliminary studies we found that high dilutions (low doses) of viral depleted HIV/MDM supernatant induced rapid calcium influx in neurons that were independent of NMDA or AMPA receptors. These results suggested that non-glutamatergic small molecules were released from infected macrophages that could influence neuronal function. In this study we identified adenosine triphosphate (ATP) and other adenine nucleotides at high concentrations in HIV/MDM supernatants. When applied onto primary neurons ATP contained in these supernatants evoked calcium flux, glutamate release, and reduced dendritic spine density by mechanisms dependent on purinergic receptors. These findings suggest a central role for ATP and purinergic receptor signaling in excitotoxicity associated with the HIV-infection of macrophages.

METHODS

Cell culture

Neuronal hippocampal cultures were prepared from Sprague Dawley rats (embryonic day 18) as previously described (Wheeler et al., 2009; Xu et al., 2011). Following hippocampi isolation, nervous tissue was trypsinized and mechanically dissociated by trituration in a calcium- and magnesium-free Hank's balanced salt solution. Neurons were plated at a density of 150,000 cells/ml on 15 mm diameter polyethylenimine-coated glass coverslips and cultured in Neurobasal media supplemented with B-27 (Invitrogen, Carlsband CA) and 1% antibiotic/antimycotic solution (104 U of penicillin G/ml, 10 mg streptomycin/ml and 25 μg amphotericin B/ml) (Gibco). Media was replaced 3 hours after plating and supplemented every 7 days with Neurobasal plus B27 media. Hippocampal cultures are >98 % neurons, as

assessed by immunofluorescent staining for MAP-2, the remainder cells are predominantly $GFAP^+$ astrocytes. Hippocampal cultures were used between 14–21 DIV. The Johns Hopkins Animal Care and Use Committee approved all procedures.

HIV-infection of monocyte derived macropahges

MDM were isolated from primary blood mononuclear cells from healthy volunteers, as previously described (Chen et al., 2002). Cells were cultured for 7 days in DMEM with 10% fetal bovine serum, 10% horse serum, 1% penicillin/streptomycin, and 1% nonessential amino acids supplemented with macrophage colony stimulating factor (100 IU/ml) in 6-well plates at a density of 1.25×10^6 cells/well. MDMs were infected with HIV-1 isolate Jago, a macrophage-tropic isolate derived from cell free CSF from a patient with confirmed HIV-associated dementia (Chen et al., 2002). Stocks of Jago were prepared in primary T-lymphocytes derived from the blood of healthy volunteers through the University of Pennsylvania Center for AIDS Research Virology Core. Jago productively infects primary T-lymphocytes and macrophages but not transformed T-cell lines (Chen et al., 2002). For infection, media was changed on day 7 and cells were inoculated with equivalent amounts of cell-free HIV-1 inoculum (100 ng p24/well). After 18 hours of incubation, cells were washed twice with PBS and incubated in fresh macrophage media. Productive HIV infection was confirmed by serial quantification of p24 antigen levels in culture supernatants by ELISA (typically of 100–400 pg/ml; NEN, Boston, MA). In control macrophage cultures, the non-nucleoside reverse transcriptase inhibitor efavirenz (EFV; 20 nM) was added 1 h before HIV inoculation. Supernatants from HIV/MDM and non-infected MDM were collected at selected time points after infection and stored at −80°C.

Calcium imaging

Cytosolic calcium levels ($[Ca^{2+}]_c$) were measured using the Ca^{2+}-specific fluorescent dye Fura-2/AM as previously described (Tovar-y-Romo et al., 2012). Briefly, hippocampal neurons were incubated for 20 min with Fura-2/AM (2 mM) at 37°C in Neurobasal media containing B27 supplement, washed with Locke's buffer (154 mM NaCl, 3.6 mM $NaHCO_3$, 5.6 mM KCl, 1 mM $MgCl_2$, 5 mM HEPES, 2.3 mM $CaCl_2$, 10 mM glucose; pH 7.4), and incubated for an additional 10 min to allow complete de-esterfication of the probe. Neurons were transferred to an RC-26 imaging chamber (Warner Instruments, Hamden CT) and maintained at 37°C (TC344B Automatic Temperature Controller; Warner instruments Hamden, CT). Continuous perfusion of neurons with Locke's buffer (2 ml/min) using a V8 channel controller (Warner Instruments, Hamden CT) allowed the rapid switching from vehicle to Locke's buffer containing different dilutions of HIV/MDM and MDM supernatants alone or in combination with inhibitors. Fura-2 inside the cells was excited at 340 and 380 nm, and emission was recorded at 510 nm with a video-based intracellular imaging system (Photon Technology Inc. Ontario, Canada) equipped with a QuantEM 512sc electron-multiplying gain camera (Photometrics Inc. Tuscon, AZ). Images were acquired at the rate of 200 ms per image-pair from neuronal somas and branches. Using reference standards, fluorescent intensities of ratio images were converted to nM $[Ca^{2+}]_c$ by curve fitting (Wheeler et al., 2009).

Immunofluorescence

Fourteen-DIV neurons were fixed with ice-cold 4% paraformaldehyde in phosphate-buffered saline (PBS) and immunostained for $P2X_4$ and $P2X_7$ and co-labeled with neuronal, pre- and post-synaptic markers. Cells were permeabilized with 0.1% Triton X-100 in tris-buffered saline (TBS-T) for 20 min at room temperature and then incubated for 1 h in blocking solution (2.5% normal goat serum and 2.5% normal horse serum in TBS-T). Cells were incubated overnight at 4°C with antibodies against $P2X_7$ (1:500, abcam, Cambridge, MA) or $P2X_4$ (1:500, Oncogene Research Products, La Jolla, CA) and MAP-2 (1:500,

Sigma), PDS95 (1:500, EMD Biosciences), or synaptophisyn (1:100, Sigma, St. Louis, MO). Neurons were washed with TBS and incubated with fluorescently tagged secondary antibodies (2 h at room temperature; Alexa Fluor 633, 546, and 488; 1:1000 dilution; Invitrogen, Grand Island, NY). Neurons were imaged with a 100X objective lens using a Zeiss Axio Observer Z1 microscope equipped with an AxioCam MRm camera and AxioVision Rel4.8 imaging software.

Cell survival

Cell viability was evaluated by assessing the number of healthy versus apoptotic nuclei using the fluorescent DNA-binding dye Hoechst 33342 as previously described (Haughey et al., 2001). Nuclei from at least 200 cells in 5 fields from 3 separate cultures per experimental condition were counted on a Zeiss Axio Observer Z1 inverted microscope (Carl Zeiss microscopy, Thornwood NY) under epifluorescence illumination (340 nm excitation and 510 nm barrier filter) using a 40X oil immersion objective. Cells were counted without knowledge of the experimental condition. Nuclei were considered apoptotic when chromatin was condensed or fragmented.

Quantification of dendritic spines

Dendritic spines were visualized by staining F-actin with Alexa 568-conjugated phalloidin. Neurons grown on glass coverslips were fixed with ice-cold 4% PFA for 20 min and then washed with PBS containing 100 mM glycine. Following a 5 min incubation in PBS containing 0.1% Triton X-100, neurons were incubated with phalloidin-568 (5 U/ml) for 30 min at room temperature. Coverslips were then washed twice with PBS and mounted on glass slides using a permanent mounting gel with anti-fading agents (Vectashield). Dendritic spines were observed using a Zeiss Axio Observer Z1 inverted microscope (Carl Zeiss microscopy Thornwood NY) under epifluorescence illumination (558 nm excitation and 568 nm emission) using a 100X oil objective. For each condition, a minimum of 10 neurons from 3 independent experiments was analyzed. The number of dendritic spines (defined as thin protrusions emerging from dendritic processes) extending from two to five primary dendrites per neuron was quantified using AxioVision 4.8.2 (Carl Zeiss Inc). Spine density was normalized to the length of the primary dendrite. Quantifications were done without knowledge of the experimental condition.

Glutamate release

Primary rat hippocampal neurons were plated in 12-well plates at a density of 250,000 cells per well. Glutamate release experiments were carried out at 14- DIV. Neurobasal media was replaced to Locke's buffer containing the glutamate transporter blocker DL-threo-beta-benzyloxyaspartate (DL-TBOA, 70 μM; Tocris) and neurons were incubated for 5 min with a 1:100 dilution of HIV/MDM or MDM supernatants. In some experimental conditions pharmacological inhibitors of purinergic receptors were added to neurons prior to incubation with HIV/MDM supernatants. Neuronal supernatants were collected and spun down at 2500 rpm for 5 min in a microcentrifuge to remove any remaining cells. Then 10 μl of supernatants or control media were combined with 40 μl of 0.1% ascorbic acid and 50 μl of a heavy standard mixture containing 1 μM deuterated [$^2H_5$] glutamic acid (CDN Isotopes, Quebec, Canada) and 0.5 μM deuterated [$^2H_3$] quinolinic acid (Synfine, Ontario, Canada). Fifty μl of −20°C acetone were added and samples were vortexed and spun down at 12,000 × g for 5 min. Samples were dried down at room temperature in a speedvac and then derivatized with 120 μl 2,2,3,3-pentafluoro-1-propanol (Sigma) and 135 μl pentafluoropropionic anhydride (Sigma). Samples were heated at 75°C for 30 min and then dried down at 50°C in a speedvac and stored at −80°C until analyzed. A matrix standard curve made in Locke's buffer with increasing amounts of glutamate (0, 0.01, 0.1, 1, and 10 μM) was prepared simultaneously with each batch of samples.

Quantification of adenine nucleotides and glutamate

For adenine nucleotides, samples (10 μl) were extracted with methanol (90 μl), vortexed, then centrifuged at 1,000 × g for 5 min at room temperature. Supernatants were analyzed by liquid chromatography coupled electrospray ionization tandem mass spectrometry (LC/ESI/MS/MS). Chromatographic separations were performed with a reverse-phase C_{18} liquid chromatography column (Phenomenex, Torrance, CA) using a programmed gradient elution with a mobile phase consisting of (A) methanol: formic acid (59:40: 1, v/v/v) with 5 mM ammonium formate to B) methanol: formic acid (99: 1, v/v) with 5 mM ammonium formate. The gradient flow rate was 0.4 ml/min with a 10 μl injection volume. Multiple reaction monitoring was performed on a LC/ESI/MS/MS (4000 Qtrap, Applied Biosystems) in positive ionization mode. Calibration standards for ATP, ADP, AMP and adenosine (Sigma-Aldrich) were prepared at the concentration range of 0.1 to 1000 ng/ml in pure methanol. Calibration curves were prepared by plotting analyte-internal standard peak area ratios vs. concentrations. The concentrations of ATP, ADP, AMP and adenosine in unknown samples were performed using a weighted least-square regression analysis of the calibration curves. Instrument control and data acquisition were performed using the Analyst 1.5.1 software.

For glutamate, GC/MS/MS was performed as previously described (Notarangelo et al., 2012). Briefly, samples were resuspended in 50 μl ethyl acetate and 1 μl was injected into an Agilent 7890A GC coupled to a 7000 MS/MS equipped with a 7693A autosampler operated in electron capture negative ionization (ECNI) mode. Methane, nitrogen and helium were used as ECNI reagent, collision and carrier gases respectively (all Airgas). The 30 m GC capillary column consisted of a 0.5 m precolumn connected to two adjoining 15 m columns (all HP-5ms with 0.25 mm ID × 0.25 μM film, Agilent). The inlet was held at 250°C and the oven temperature initially held at 60°C for 1 min and then ramped 13°C/min to 230°C for a total run time of 14 min. The following multiple reaction monitoring transitions were optimized from transitions previously described (Eckstein et al., 2008); glutamate Q1 = 537.2, Q3 = 313.0, CE = 15V, RT = 7.7 min; [$^2H_5$] glutamate Q1 = 542.2, Q3 = 314.0, CE = 10V, RT = 7.7 min. Samples were injected twice and peak areas were averaged and normalized to heavy standards. Data were analyzed with Agilent MassHunter software, Build B.04. Values were fit to the matrix-spiked standard curve and corrected for the appropriate dilution factor.

RESULTS

High dilution HIV/MDM supernatants rapidly activate calcium permeable P2X receptors on neurons

Exposure of cultured rat hippocampal neurons to mock-infected MDM and HIV/MDM supernatants (1:1 – 1:1000) induced cytosolic Ca^{2+} increases in a dose-dependent manner (Fig. 1A). HIV/MDM supernatants evoked a transient increase in cytosolic calcium. Supernatants from HIV/MDM were several orders of magnitude more potent to induce $[Ca^{2+}]_c$ increases compared with control MDM supernatants. HIV/MDM did not evoke $[Ca^{2+}]_c$ responses in calcium free buffer, suggesting that HIV/MDM induced the influx of extracellular calcium (Fig. 1A).

To identify the mechanism for HIV/MDM-evoked $[Ca^{2+}]_c$ increases, we blocked specific Ca^{2+} permeable receptors with selective pharmacological antagonists. High dilutions (1:500) of HIV/MDM supernatants evoked rapid $[Ca^{2+}]_c$ responses in neurons that were not modified in the presence of NMDA antagonist MK-801 (10 μM), AMPA antagonist NBQX (10 μM), or L-type voltage-operated calcium channels blocker nifedipine (10 μM) (Fig 2A, B). However, two general antagonists of P2X type purinergic receptors, PPADS (10 μM) and suramin (100 μM), completely blocked HIV/MDM supernatant-stimulated $[Ca^{2+}]_c$

responses. We then tested selective inhibitors for two P2X receptor subtypes known to have a high permeability for calcium. The $P2X_7$ antagonist AZ10606120 (10 μM), and $P2X_4$ antagonist 5-BDBD (10 μM) each reduced the $[Ca^{2+}]_c$ responses by approximately half. Combined, these antagonists produced a near complete block of HIV/MDM supernatant-induced increase of $[Ca^{2+}]_c$ (Fig 2A, B). Finally, we pre-incubated HIV/MDM supernatant with apyrase (2U/10 μl), an enzyme with ATPase catalytic activity, and found that ATP-depleted HIV/MDM supernatants did not induce $[Ca^{2+}]_c$ influx when applied onto neurons. These data suggest that ATP or other adenine nucleotides present in HIV/MDM supernatants evoked rapid calcium increases in neurons through ligation of calcium permeable P2X receptors.

Hippocampal neurons express $P2X_4$ and $P2X_7$ receptors

The expression of $P2X_4$ and $P2X_7$ in our hippocampal neuronal cultures was confirmed by double-immunofluorescence for each P2X receptor subtype and the neuronal marker MAP-2 (Fig. 3A–B). $P2X_4$ and $P2X_7$ co-localized with the postsynaptic marker PSD-95 (Fig. 3C–D), but not with the presynaptic marker synaptophysin (Fig. 3E–F), indicating the expression of both receptors at postsynaptic sites on neurons.

HIV/MDM supernatants contain high concentrations of adenine nucleotides

We directly measured the concentrations of adenine nucleotides and glutamate in MDM and HIV/MDM supernatants by HPLC- and GC-mass spectrometry. In HIV/MDM and MDM adenosine was near or below detectable levels. In HIV/MDM the concentration of ATP was 68.2 ± 1.9 μM, ADP was 18.4 ±3.2 μM, and AMP was 27.0 ± 8.5 μM (Table 1). Compared with MDM supernatants, the concentrations of AMP, ADP and ATP were 4–7 times greater in supernatants from HIV/MDM, consistent with potency for each of these supernatants to evoke calcium flux in neurons. Concentrations of glutamate were 4.07 ± 0.05 μM for HIV/MDM, and 2.35 ± 0.03 μM for MDM, consistent with a sub-threshold concentration of glutamate to evoke an NMDA-mediated calcium response at these low dilutions (all concentrations were calculated for a 1:100 dilution of supernatants used in these experiments).

ATP in HIV/MDM supernatant induces neuronal damage

It has been demonstrated that HIV/MDM supernatants are toxic to neurons by mechanisms that involve NMDA receptor activation (O'Donnell et al., 2006). Since blockade of NMDA and AMPA receptors was unable to blunt rapid $[Ca^{2+}]_c$ responses to HIV/MDM supernatants, we next determined if blockade of purinergic receptors could protect neurons from the toxic effects of HIV/MDM. We exposed neurons to MDM or HIV/MDM supernatants for 24 h and quantified the number of apoptotic nuclei using the DNA binding dye Hoechst 33342. Nuclei with diffusely stained chromatin were considered healthy, and nuclei with condensed or fragmented chromatin were considered apoptotic. We found that neuronal viability was reduced by MDM and HIV/MDM supernatants in a dose-dependent manner, and HIV/MDM supernatants were more potent inducers of neuronal death compared with MDM (Figure 4). The frequency of apoptotic nuclei in 1:100 HIV/MDM supernatant-treated cultures was reduced by degradation of ATP with apyrase (2 IU/10 μl HIV/MDM), general inhibition of P2X with PPADS (10 uM), or suramin (100 μM), by specific antagonists of $P2X_7$ (AZ10606120; 10 μM), $P2X_4$ (5-BDBD; 10 μM), and an AMPA receptor antagonist (NBQX; 10 μM). Near complete protection was afforded by antagonizing NMDA receptors (MK-801; 10 μM).

Given that synaptic damage rather than frank neuronal loss is more commonly observed in HIV-infected individuals, we determined whether very low concentrations of HIV/MDM supernatants could damage dendritic spines by mechanisms that involved purinergic or

glutaminergic receptors. High dilutions (1:250) of HIV/MDM but not MDM supernatants produced considerable damage to dendritic spines (Fig 5A, B). Degradation of extracellular ATP with apyrase (2 IU/10 μl HIV/MDM), and general antagonists of purinergic receptors (PPADS; 10 μM, or suramin; 100 μM) partially protected dendritic spines from HIV/MDM supernatant-induced damage. Specific antagonists of $P2X_4$ (5-BDBD; 10 μM) and $P2X_7$ (AZ10606120; 10 μM), alone or combined conferred a significant, but not complete, protection. Likewise, an antagonist of AMPA (NBQX, 10 μM) provided partial protection. Complete dendritic branch protection was only achieved by NMDA receptor blockade (10 μM MK-801) (Fig 5B). These data demonstrate that a very low concentration of HIV/MDM supernatants can cause considerable damage to dendritic spines by mechanisms that involve calcium permeable P2X and NMDA receptors.

HIV/MDM supernatants trigger the release of glutamate from neurons by activating purinergic receptors

Our findings that damage to dendritic spines induced by HIV/MDM supernatants could be blocked with an NMDA receptor antagonist are consistent with previous a report showing that NMDA receptors are key players in HIV/MDM induced neuronal death/damage (O'Donnell et al., 2006). However, our current studies demonstrate that low concentrations of HIV/MDM supernatants rapidly evoke a P2X receptor mediated response without any immediate contribution by NMDA receptors. Given these differential findings, we thought it possible that adenine nucleotides in HIV/MDM supernatants activated a P2-mediated release of glutamate from neurons. To test this hypothesis we exposed neurons to HIV/MDM or MDM supernatants for 5 min and measured glutamate in the media. HIV/MDM, but not MDM supernatants induced a ~2.5-fold increase in extracellular glutamate over baseline (after controlling for glutamate contained in supernatants; Fig 6). This HIV/MDM supernatant-evoked release of glutamate was blocked by a general antagonist of purinergic receptors (PPADS; 10 μM) but not by selective blockade of $P2X_4$ and $P2X_7$ (Fig 6). These data suggest calcium impermeable P2X, or metabotropic P2Y receptors contribute to the release of glutamate induced by adenine nucleotides contained in HIV/MDM supernatants.

DISCUSSION

The transmigration of HIV-infected macrophages into brain constitutes a route for virus entry into the CNS, and may represent a reservoir for latent virus (Fischer-Smith et al., 2008; Thompson et al., 2011). These HIV-infected macrophages are thought to contribute to the development of HAND through the release of virus, and cellular metabolites that can cause harm to neighboring cells. Glutamate and related amino acids that are released from HIV-infected macrophages can cause damage or induce the death of neurons through hyper-activation of calcium permeable NMDA and AMPA receptors (Brew et al., 1995; Jiang et al., 2001; Valle et al., 2004; O'Donnell et al., 2006). In this study we found that low dilutions of HIV/MDM were highly toxic to neurons. Higher dilutions of HIV/MDM supernatants evoked calcium influxes when applied onto cultured neurons that were independent of AMPA or NMDA receptor antagonists. These high dilutions of HIV/MDM did not induce neuronal death, but downregulated the density of dendritic spines. We determined that these calcium fluxes were mediated by purinergic receptors activated by ATP, which was found at high concentrations in HIV/MDM supernatants. These high dilution HIV/MDM supernatants did not themselves contain sufficient amounts of glutamate to activate NMDA or AMPA mediated calcium flux, but evoked the release of glutamate from neurons by mechanisms dependent on calcium impermeable P2X receptors or metabotropic P2Y receptors. Since calcium does not appear to be involved, this would suggest that glutamate was released through non-synaptic mechanisms, or though a mechanism that decreased the uptake or breakdown of glutamate. The downregulation of

dendritic spines was rescued by blockade of NMDA receptors or purinergic receptors. Thus, excitotoxic damage to neurons by HIV/MDM may involve disturbances in glutamate handling that are induced by the release of ATP from macrophages, and purinergic receptor activation on neurons. Further study to identify the exact mechanisms responsible by which ATP contained in HIV/MDM modifies glutamate handling in neurons could identify novel targets for neuroprotection in HIV infected individuals.

In addition to roles in energy metabolism, ATP and other adenine nucleotides function as extracellular signaling molecules. Extracellular ATP activates a family of purinergic receptors broadly classified into P2X (ligand-gated cation channels), and P2Y (G-protein coupled). There are numerous family members within each class of P2X and P2Y receptors that show differential sensitivity to activation by ATP, desensitization rates, cellular expression, and linkages to downstream effector pathways. Hence, the P2 family of receptors regulates a wide variety of biological responses (see (Khakh and North, 2012; Weisman et al., 2012)for recent reviews). In the CNS, ATP appears to function largely as modulator of neuronal activity rather than a fast-acting neurotransmitter. Activation of P2 receptors on neurons regulates glutamatergic transmission. For example long-term potentiation (LTP) induced by ATP can be blocked by co-application of an NMDA receptor antagonist, but is not blocked by antagonists of P2X or P2Y receptors (Fujii et al., 2002). ATP appears to regulate LTP through pre- and postsynaptic effects that modulate the threshold for LTP in a concentration dependent manner (Wang et al., 2002). Low concentrations of ATP suppress inhibitory tone, and enhance the excitability of neuronal circuits (Lee et al., 2013). Higher concentrations of ATP regulate NMDA receptor activity at low firing frequencies to increase the threshold for induction of LTP (Pankratov et al., 2002). These findings combined with our current data suggest that the infiltration of HIV-infected macrophages into brain could depress neuronal tone through mechanisms that involve excessive release of ATP from macrophages, and the effects of ATP on purinergic signaling and glutamate handling on neurons. Indeed, we found that high dilutions of HIV/MDM supernatants applied onto cultured hippocampal neurons decreased dendritic spine density by mechanisms dependent on purinergic and NMDA receptor activity. These findings are similar to neuropathological observations that have shown decreased spine density in HIV-infected subjects (Sa et al., 2004). The effects of ATP released from HIV-infected macrophages on spine density may be augmented by exposure to HIV proteins such as gp120 or Tat, or by opiate abuse, that have each been shown to reduce dendritic spine density (Fitting et al., 2010; Bandaru et al., 2011). We detected multiple forms of adenine nucleotides in HIV/MDM, and it is likely that these other purines contribute to effects of HIV-infection on CNS function.

Extracellular ATP functions as a chemotactic and pro-inflammatory mediator that regulates the macrophage response to pathogens and tissue damage. ATP released by dead or dying cells, or from macrophages themselves (autocrine signaling) directs macrophages to sites of tissue damage (Ayna et al., 2012) (Kronlage et al., 2010) (Elliott et al., 2009), and regulates the NLRP3 inflammasome, a protein complex involved in IL-1β and IL-18 processing and release (Gombault et al., 2012; Riteau et al., 2012). The mechanism for ATP release from macrophages requires the hemichannel pannexin-1 (Qu et al., 2011; Riteau et al., 2012), although alternative release mechanisms involving voltage-dependent ion channels or exocytosis of intracellular vesicles (exosomes) containing ATP may also be involved (Fitz, 2007). The release of ATP from macrophages and T-cells is induced by binding of the envelope protein gp120 (Seror et al., 2011; Hazleton et al., 2012). This extracellular ATP acts through purinergic receptors and proline-rich tyrosine kinase 2 to induce a transient plasma membrane depolarization that facilitates fusion between HIV and host cell membranes (Seror et al., 2011). Blockade of purinergic receptors prevents productive HIV-1 infection, demonstrating a critical role for extracellular ATP in the viral lifecycle (Hazleton

et al., 2012). Thus, the release of ATP from HIV-infected macrophages appears to be a host response to pathogen exposure that is required for infection, and in the CNS may damage or down-regulate dendritic spines on proximal neurons.

Based on the results presented here, we suggest that HIV-infected perivascular macrophages contribute to the neurocognitive deficits seen in HAND through the release of ATP that acts on purinergic receptors to dysregulate glutamatergic signaling, and reduce dendritic spine density on neurons. Purinergic receptor modulation of glutamate release is known to occur in astrocytes (Sperlágh et al., 2002; Duan et al., 2003; Fellin et al., 2006). Thus, the release of ATP from infiltrating HIV-infected macrophages could increase glutamatergic tone through actions mediated by purinergic receptors. While clinical trials testing NMDA antagonists have yet to show success at improving cognitive functions, pharmacological targeting of purinergic receptors may indirectly reduce excitotoxic damage associated with the infiltration of HIV-infected macrophages to the CNS. A number of purinergic receptor antagonists are being tested in clinical trials for rheumatoid arthritis, chronic pain and inflammation (see (Gum et al., 2012) for review). The compounds may soon be available and could be useful for treating secondary neuronal damage in HIV-infected individuals.

Acknowledgments

The authors would like to acknowledge Carrie Berlett for her technical support. This study was supported by NIH grants AA0017408, MH077542 and AG034849 to NJH.

LIST OF ABBREVIATIONS

5-BDBD	5-(3-bromophenyl)-1,3-dihydro-2H-benzofuro[3,2-e]-1,4-diazepin-2-one
ADP	adenosine diphosphate
AMP	adenosine monophosphate
AMPA	α-amino-3-hydroxy-5-methyl-isoxazol-4-yl propionate
ATP	adenosine triphosphate
AZ10606120	N-[2-[[2-[(2-Hydroxyethyl)amino]ethyl]amino]-5-quinolinyl]-2-tricyclo[3.3.1.13,7]dec-1-ylacetamide dihydrochloride
cART	combination antiretroviral therapy
DIV	days in vitro
DL-TBOA	DL-threo-β-Benzyloxyaspartic acid
ECNI	electron capture negative ionization
GC	gas chromatography
HAND	HIV-associated neurocognitive disorder
HIV	human immunodeficiency virus
HIV/MDM	HIV-infected monocyte derived macrophage
MDM	monocyte derived macrophage
MK-801	5-Methyl-10,11-dihydro-5*H*-dibenzo[*a,d*]cyclohepten-5,10-imine maleate
MS	mass spectrometry
NBQX	2,3-dioxo-6-nitro-1,2,3,4-tetrahydrobenzo[f]quinoxaline-7-sulfonamide
NMDA	N-methyl-D-aspartate

PBS	phosphate-buffered saline
PPADS	pyridoxal phosphate-6-azophenyl-2'-4'-disulphonic acid
TBS	tris-buffered saline

References

Ayna G, Krysko DV, Kaczmarek A, Petrovski G, Vandenabeele P, Fesus L. ATP release from dying autophagic cells and their phagocytosis are crucial for inflammasome activation in macrophages. PLoS One. 2012; 7:e40069. [PubMed: 22768222]

Bandaru VV, Patel N, Ewaleifoh O, Haughey NJ. A Failure to Normalize Biochemical and Metabolic Insults During Morphine Withdrawal Disrupts Synaptic Repair in Mice Transgenic for HIV-gp120. J Neuroimmune Pharmacol. 2011; 6:640–649. [PubMed: 21748284]

Brew BJ, Corbeil J, Pemberton L, Evans L, Saito K, Penny R, Cooper DA, Heyes MP. Quinolinic acid production is related to macrophage tropic isolates of HIV-1. J Neurovirol. 1995; 1:369–374. [PubMed: 9222379]

Buckner CM, Calderon TM, Willams DW, Belbin TJ, Berman JW. Characterization of monocyte maturation/differentiation that facilitates their transmigration across the blood-brain barrier and infection by HIV: implications for NeuroAIDS. Cell Immunol. 2011; 267:109–123. [PubMed: 21292246]

Chen W, Sulcove J, Frank I, Jaffer S, Ozdener H, Kolson DL. Development of a human neuronal cell model for human immunodeficiency virus (HIV)-infected macrophage-induced neurotoxicity: apoptosis induced by HIV type 1 primary isolates and evidence for involvement of the Bcl-2/Bcl-xL-sensitive intrinsic apoptosis pathway. J Virol. 2002; 76:9407–9419. [PubMed: 12186923]

Dreyer EB, Lipton SA. The coat protein gp120 of HIV-1 inhibits astrocyte uptake of excitatory amino acids via macrophage arachidonic acid. Eur J Neurosci. 1995; 7:2502–2507. [PubMed: 8845955]

Duan S, Anderson CM, Keung EC, Chen Y, Swanson RA. P2×7 receptor-mediated release of excitatory amino acids from astrocytes. J Neurosci. 2003; 23:1320–1328. [PubMed: 12598620]

Eckstein JA, Ammerman GM, Reveles JM, Ackermann BL. Simultaneous profiling of multiple neurochemical pathways from a single cerebrospinal fluid sample using GC/MS/MS with electron capture detection. J Mass Spectrom. 2008; 43:782–790. [PubMed: 18286669]

Elliott MR, Chekeni FB, Trampont PC, Lazarowski ER, Kadl A, Walk SF, Park D, Woodson RI, Ostankovich M, Sharma P, Lysiak JJ, Harden TK, Leitinger N, Ravichandran KS. Nucleotides released by apoptotic cells act as a find-me signal to promote phagocytic clearance. Nature. 2009; 461:282–286. [PubMed: 19741708]

Erdmann N, Tian C, Huang Y, Zhao J, Herek S, Curthoys N, Zheng J. In vitro glutaminase regulation and mechanisms of glutamate generation in HIV-1-infected macrophage. J Neurochem. 2009; 109:551–561. [PubMed: 19222703]

Erdmann N, Zhao J, Lopez AL, Herek S, Curthoys N, Hexum TD, Tsukamoto T, Ferraris D, Zheng J. Glutamate production by HIV-1 infected human macrophage is blocked by the inhibition of glutaminase. J Neurochem. 2007; 102:539–549. [PubMed: 17596215]

Everall I, Vaida F, Khanlou N, Lazzaretto D, Achim C, Letendre S, Moore D, Ellis R, Cherner M, Gelman B, Morgello S, Singer E, Grant I, Masliah E. Cliniconeuropathologic correlates of human immunodeficiency virus in the era of antiretroviral therapy. J Neurovirol. 2009; 15:360–370. [PubMed: 20175693]

Fellin T, Pozzan T, Carmignoto G. Purinergic receptors mediate two distinct glutamate release pathways in hippocampal astrocytes. J Biol Chem. 2006; 281:4274–4284. [PubMed: 16338906]

Fischer-Smith T, Bell C, Croul S, Lewis M, Rappaport J. Monocyte/macrophage trafficking in acquired immunodeficiency syndrome encephalitis: lessons from human and nonhuman primate studies. J Neurovirol. 2008; 14:318–326. [PubMed: 18780233]

Fitting S, Xu R, Bull C, Buch SK, El-Hage N, Nath A, Knapp PE, Hauser KF. Interactive comorbidity between opioid drug abuse and HIV-1 Tat: chronic exposure augments spine loss and sublethal dendritic pathology in striatal neurons. Am J Pathol. 2010; 177:1397–1410. [PubMed: 20651230]

Fitz JG. Regulation of cellular ATP release. Trans Am Clin Climatol Assoc. 2007; 118:199–208. [PubMed: 18528503]

Fujii S, Kato H, Kuroda Y. Cooperativity between extracellular adenosine 5'-triphosphate and activation of N-methyl-D-aspartate receptors in long-term potentiation induction in hippocampal CA1 neurons. Neuroscience. 2002; 113:617–628. [PubMed: 12150781]

Gombault A, Baron L, Couillin I. ATP release and purinergic signaling in NLRP3 inflammasome activation. Front Immunol. 2012; 3:414. [PubMed: 23316199]

Gras G, Kaul M. Molecular mechanisms of neuroinvasion by monocytes-macrophages in HIV-1 infection. Retrovirology. 2010; 7:30. [PubMed: 20374632]

Gum RJ, Wakefield B, Jarvis MF. P2X receptor antagonists for pain management: examination of binding and physicochemical properties. Purinergic Signal. 2012; 8:41–56. [PubMed: 22086553]

Haughey NJ, Nath A, Mattson MP, Slevin JT, Geiger JD. HIV-1 Tat through phosphorylation of NMDA receptors potentiates glutamate excitotoxicity. J Neurochem. 2001; 78:457–467. [PubMed: 11483648]

Hazleton JE, Berman JW, Eugenin EA. Purinergic receptors are required for HIV-1 infection of primary human macrophages. J Immunol. 2012; 188:4488–4495. [PubMed: 22450808]

Heaton RK, et al. HIV-associated neurocognitive disorders persist in the era of potent antiretroviral therapy: CHARTER Study. Neurology. 2010; 75:2087–2096. [PubMed: 21135382]

Heaton RK, et al. HIV-associated neurocognitive disorders before and during the era of combination antiretroviral therapy: differences in rates, nature, and predictors. J Neurovirol. 2011; 17:3–16. [PubMed: 21174240]

Hult B, Chana G, Masliah E, Everall I. Neurobiology of HIV. Int Rev Psychiatry. 2008; 20:3–13. [PubMed: 18240058]

Jiang ZG, Piggee C, Heyes MP, Murphy C, Quearry B, Bauer M, Zheng J, Gendelman HE, Markey SP. Glutamate is a mediator of neurotoxicity in secretions of activated HIV-1-infected macrophages. J Neuroimmunol. 2001; 117:97–107. [PubMed: 11431009]

Khakh BS, North RA. Neuromodulation by extracellular ATP and P2X receptors in the CNS. Neuron. 2012; 76:51–69. [PubMed: 23040806]

Koenig S, Gendelman HE, Orenstein JM, Dal Canto MC, Pezeshkpour GH, Yungbluth M, Janotta F, Aksamit A, Martin MA, Fauci AS. Detection of AIDS virus in macrophages in brain tissue from AIDS patients with encephalopathy. Science. 1986; 233:1089–1093. [PubMed: 3016903]

Kraft-Terry SD, Buch SJ, Fox HS, Gendelman HE. A coat of many colors: neuroimmune crosstalk in human immunodeficiency virus infection. Neuron. 2009; 64:133–145. [PubMed: 19840555]

Kronlage M, Song J, Sorokin L, Isfort K, Schwerdtle T, Leipziger J, Robaye B, Conley PB, Kim HC, Sargin S, Schon P, Schwab A, Hanley PJ. Autocrine purinergic receptor signaling is essential for macrophage chemotaxis. Sci Signal. 2010; 3 ra55.

Langford TD, Letendre SL, Larrea GJ, Masliah E. Changing patterns in the neuropathogenesis of HIV during the HAART era. Brain Pathol. 2003; 13:195–210. [PubMed: 12744473]

Lee HU, Yamazaki Y, Tanaka KF, Furuya K, Sokabe M, Hida H, Takao K, Miyakawa T, Fujii S, Ikenaka K. Increased astrocytic ATP release results in enhanced excitability of the hippocampus. Glia. 2013; 61:210–224. [PubMed: 23018918]

McArthur JC, Steiner J, Sacktor N, Nath A. Human immunodeficiency virus-associated neurocognitive disorders: Mind the gap. Ann Neurol. 2010; 67:699–714. [PubMed: 20517932]

Notarangelo FM, Wu HQ, Macherone A, Graham DR, Schwarcz R. Gas chromatography/tandem mass spectrometry detection of extracellular kynurenine and related metabolites in normal and lesioned rat brain. Anal Biochem. 2012; 421:573–581. [PubMed: 22239963]

O'Donnell LA, Agrawal A, Jordan-Sciutto KL, Dichter MA, Lynch DR, Kolson DL. Human immunodeficiency virus (HIV)-induced neurotoxicity: roles for the NMDA receptor subtypes. J Neurosci. 2006; 26:981–990. [PubMed: 16421318]

Qu Y, Misaghi S, Newton K, Gilmour LL, Louie S, Cupp JE, Dubyak GR, Hackos D, Dixit VM. Pannexin-1 is required for ATP release during apoptosis but not for inflammasome activation. J Immunol. 2011; 186:6553–6561. [PubMed: 21508259]

Riteau N, Baron L, Villeret B, Guillou N, Savigny F, Ryffel B, Rassendren F, Le Bert M, Gombault A, Couillin I. ATP release and purinergic signaling: a common pathway for particle-mediated inflammasome activation. Cell Death Dis. 2012; 3:e403. [PubMed: 23059822]

Sa MJ, Madeira MD, Ruela C, Volk B, Mota-Miranda A, Paula-Barbosa MM. Dendritic changes in the hippocampal formation of AIDS patients: a quantitative Golgi study. Acta Neuropathol. 2004; 107:97–110. [PubMed: 14605830]

Seror C, et al. Extracellular ATP acts on P2Y2 purinergic receptors to facilitate HIV-1 infection. J Exp Med. 2011; 208:1823–1834. [PubMed: 21859844]

Sperlágh B, Kofalvi A, Deuchars J, Atkinson L, Milligan CJ, Buckley NJ, Vizi ES. Involvement of P2×7 receptors in the regulation of neurotransmitter release in the rat hippocampus. J Neurochem. 2002; 81:1196–1211. [PubMed: 12068068]

Thompson KA, Cherry CL, Bell JE, McLean CA. Brain cell reservoirs of latent virus in presymptomatic HIV-infected individuals. Am J Pathol. 2011; 179:1623–1629. [PubMed: 21871429]

Tian C, Sun L, Jia B, Ma K, Curthoys N, Ding J, Zheng J. Mitochondrial glutaminase release contributes to glutamate-mediated neurotoxicity during human immunodeficiency virus-1 infection. J Neuroimmune Pharmacol. 2012; 7:619–628. [PubMed: 22527635]

Tovar-y-Romo LB, Bumpus NN, Pomerantz D, Avery LB, Sacktor N, McArthur JC, Haughey NJ. Dendritic spine injury induced by the 8-hydroxy metabolite of efavirenz. J Pharmacol Exp Ther. 2012; 343:696–703. [PubMed: 22984227]

Valle M, Price RW, Nilsson A, Heyes M, Verotta D. CSF quinolinic acid levels are determined by local HIV infection: cross-sectional analysis and modelling of dynamics following antiretroviral therapy. Brain. 2004; 127:1047–1060. [PubMed: 15013955]

Vivithanaporn P, Heo G, Gamble J, Krentz HB, Hoke A, Gill MJ, Power C. Neurologic disease burden in treated HIV/AIDS predicts survival: a population-based study. Neurology. 2010; 75:1150–1158. [PubMed: 20739646]

Weisman GA, Camden JM, Peterson TS, Ajit D, Woods LT, Erb L. P2 receptors for extracellular nucleotides in the central nervous system: role of P2×7 and P2Y(2) receptor interactions in neuroinflammation. Mol Neurobiol. 2012; 46:96–113. [PubMed: 22467178]

Wheeler D, Knapp E, Bandaru VV, Wang Y, Knorr D, Poirier C, Mattson MP, Geiger JD, Haughey NJ. Tumor necrosis factor-alpha-induced neutral sphingomyelinase-2 modulates synaptic plasticity by controlling the membrane insertion of NMDA receptors. J Neurochem. 2009; 109:1237–1249. [PubMed: 19476542]

Xu H, Bae M, Tovar-y-Romo LB, Patel N, Bandaru VV, Pomerantz D, Steiner JP, Haughey NJ. The human immunodeficiency virus coat protein gp120 promotes forward trafficking and surface clustering of NMDA receptors in membrane microdomains. J Neurosci. 2011; 31:17074–17090. [PubMed: 22114277]

Yadav A, Collman RG. CNS inflammation and macrophage/microglial biology associated with HIV-1 infection. J Neuroimmune Pharmacol. 2009; 4:430–447. [PubMed: 19768553]

Yao H, Bethel-Brown C, Li CZ, Buch SJ. HIV neuropathogenesis: a tight rope walk of innate immunity. J Neuroimmune Pharmacol. 2010; 5:489–495. [PubMed: 20354805]

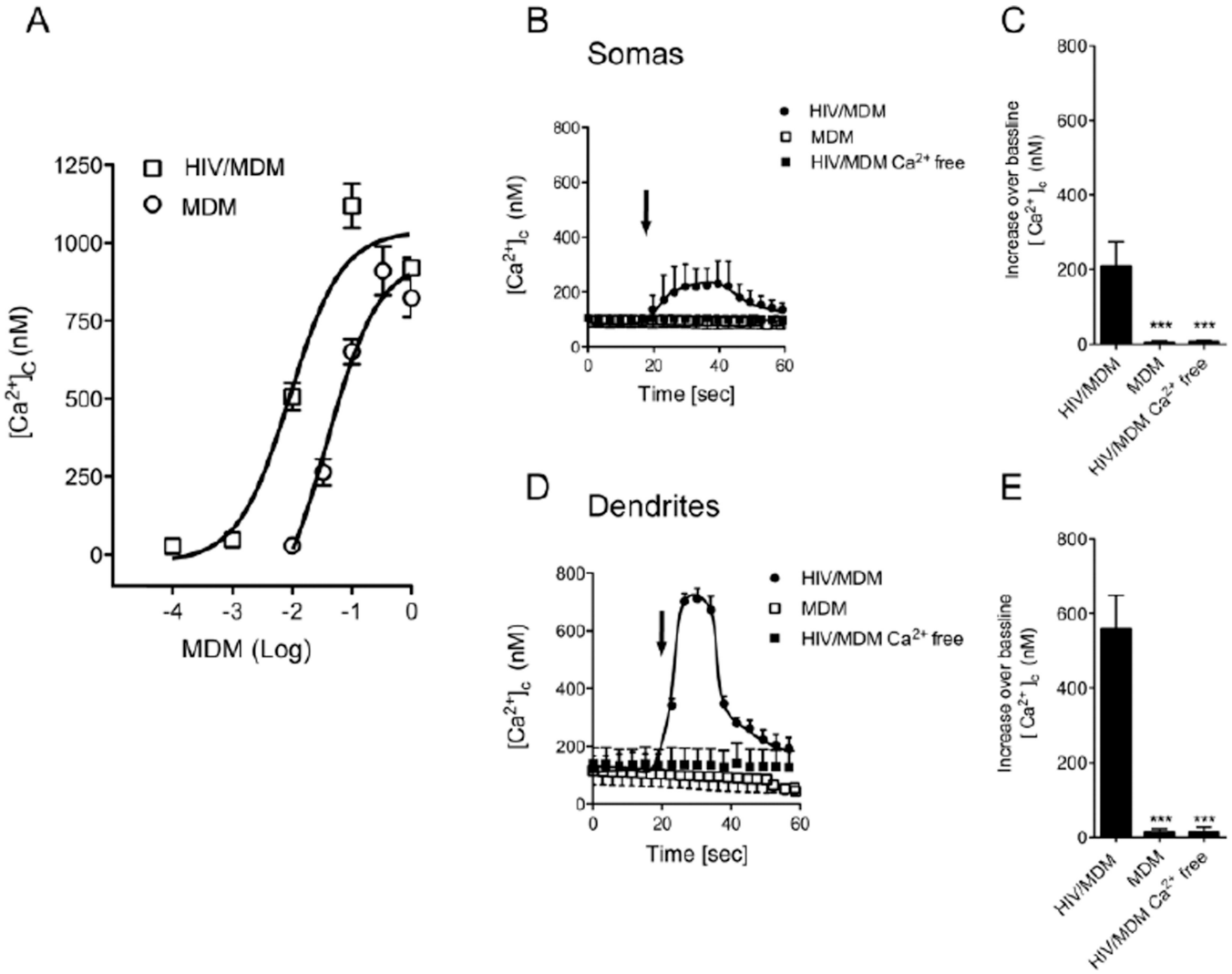

Figure 1. HIV/MDM supernatants stimulate extracellular calcium influx in cultured hippocampal neurons

MDM and HIV/MDM supernatants evoked dose-dependent increases of $[Ca^{2+}]_c$ in primary hippocampal neurons. **(A)** Peak $[Ca^{2+}]_c$ increases over baseline in neurons exposed to the indicated concentrations of supernatants from MDM and HIV/MDM. HIV/MDM evoked larger $[Ca^{2+}]_c$ increases compared with MDM at all concentrations tested. Representative traces showing the time course and peak $[Ca^{2+}]_c$ increases over baseline evoked by brief applications of supernatants from MDM, HIV-MDM, and HIV/MDM in calcium free buffer for neuronal somas **(B–C)** and dendrites **(D–E)**. MDM and HIV/MDM supernatants were each used at 1:500 dilution (arrows indicate time of addition). Each data point represents the average ± SD of 10–12 somas or 25–30 dendrites derived from 7 separate experiments. ANOVA with Tukey's post hoc comparisons. *** $p < 0.001$.

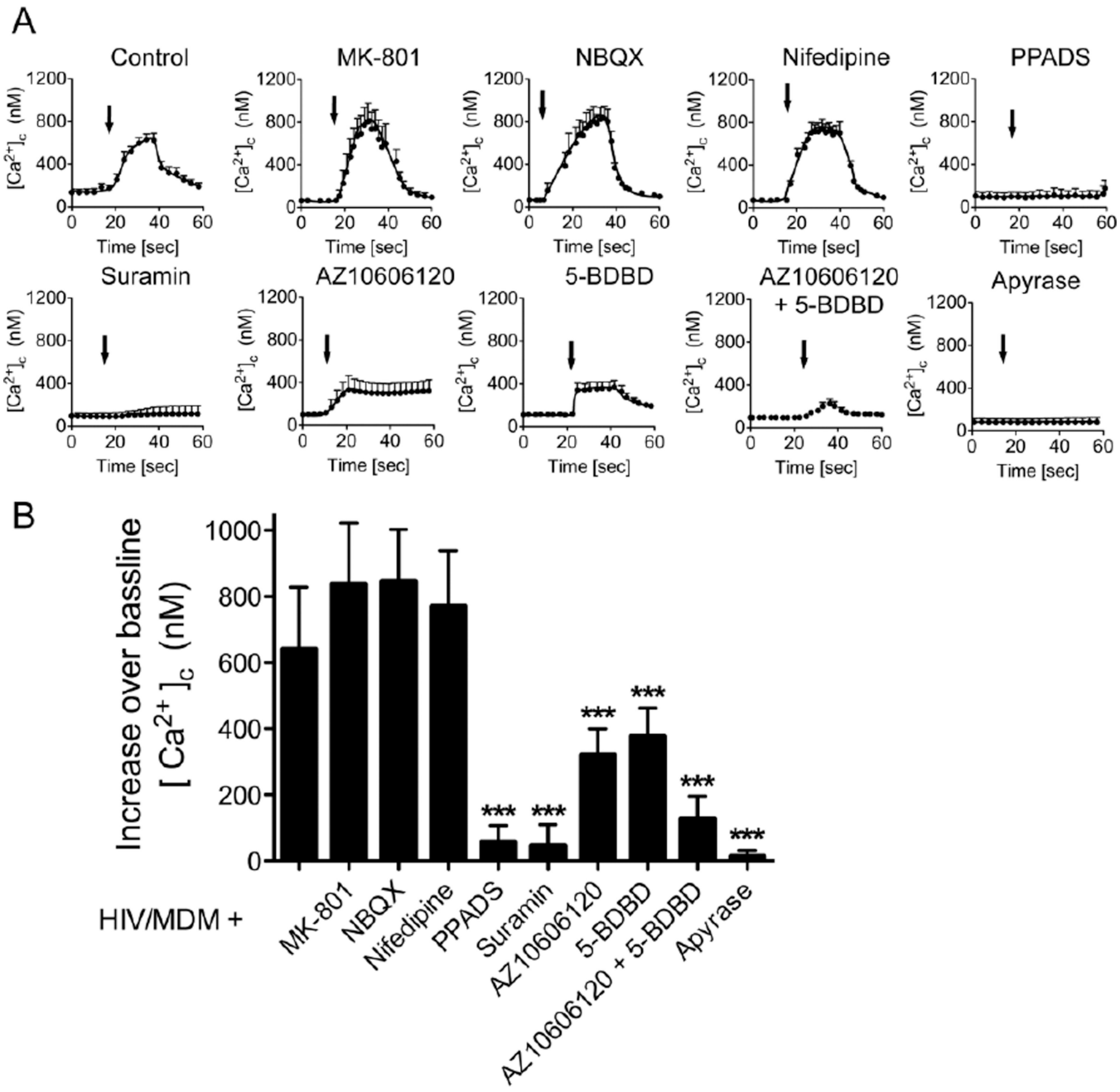

Figure 2. HIV/MDM activates calcium permeable purinergic receptors

HIV/MDM-evoked calcium flux was quantified in the presence of the indicated calcium channel antagonists. **(A)** Representative traces showing low dose HIV/MDM (1:500)-evoked $[Ca^{2+}]_c$ responses in neuronal dendrites in the presence of vehicle (Control), or antagonists for NMDA (MK-801; 10 μM), AMPA (NBQX; 10 μM), L-type voltage operated calcium channels (Nifedipine; 10 μM), general blockers of calcium permeable P2X receptors (PPADS: 10 μM. Suramin; 100 μM), $P2X_7$ (AZ10606120; 10 μM), $P2X_4$ (5-BDBD; 10 μM), and HIV/MDM supernatants pre-incubated with apyrase (2U/10 μl). **(B)** Summary data showing peak amplitudes of $[Ca^{2+}]_c$ responses for the indicated conditions. Data are the average ± SD of $[Ca^{2+}]_c$ responses recorded from 30–35 dendrites in 7 independent experiments. ANOVA with Tukey's post hoc comparisons. *** $p < 0.001$.

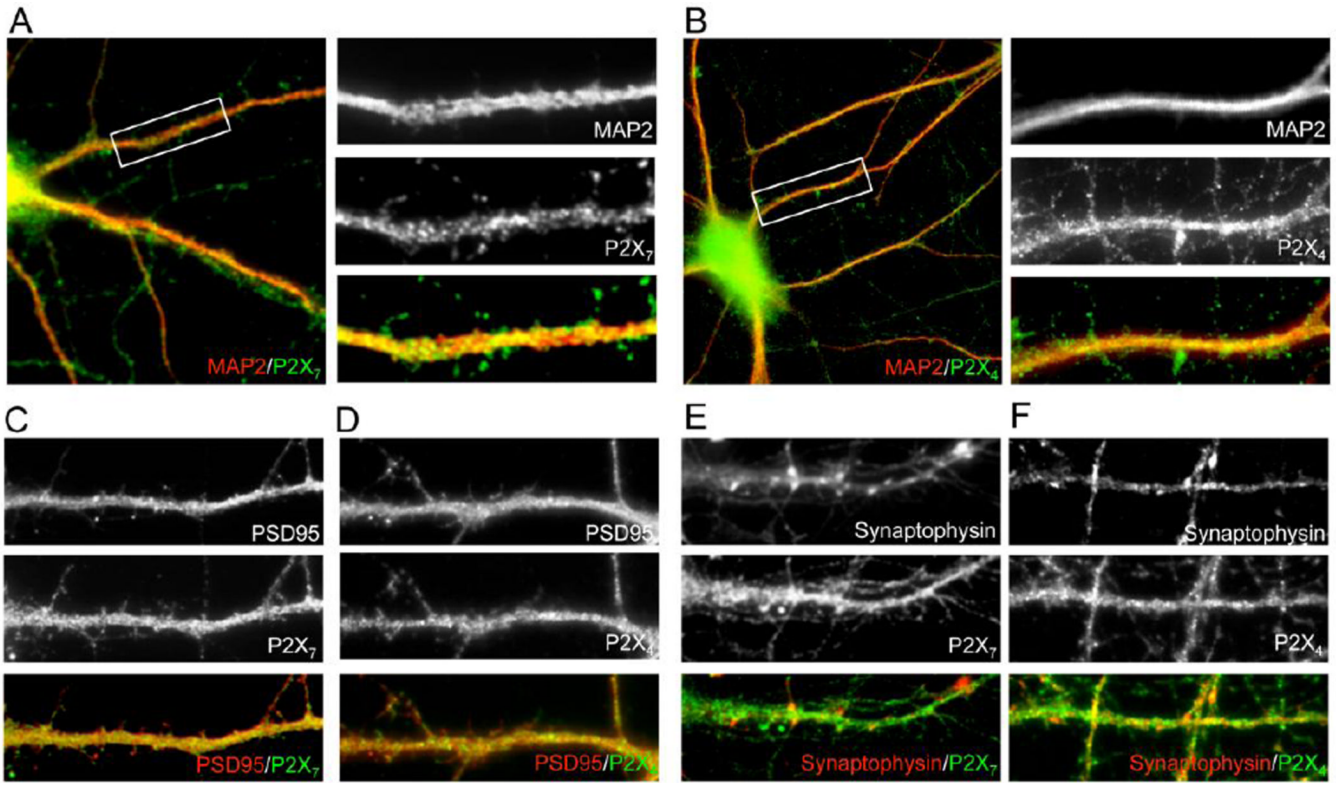

Figure 3. The purinergic receptors $P2X_7$ and $P2X_4$ are expressed at post-synaptic regions in hippocampal neurons

Representative images showing the expression of $P2X_7$ and $P2X_4$ in hippocampal neurons. Co-localization of $P2X_7$**(A)** and $P2X_4$**(B)** with the neuronal marker MAP-2. Images to the right of each primary image are enlarged to show the indicated portion of the dendrite. MAP-2 (red) and $P2X_4$ or $P2X_7$ (green) appear as yellow in the merged images when co-localized with MAP-2. $P2X_7$**(C)** and $P2X_4$**(D)**(green) co-localize with the postsynaptic marker PSD-9 (red). $P2X_7$**(E)** and $P2X_4$**(F)** (green) do not co-localize with the presynaptic marker synaptophysin (red).

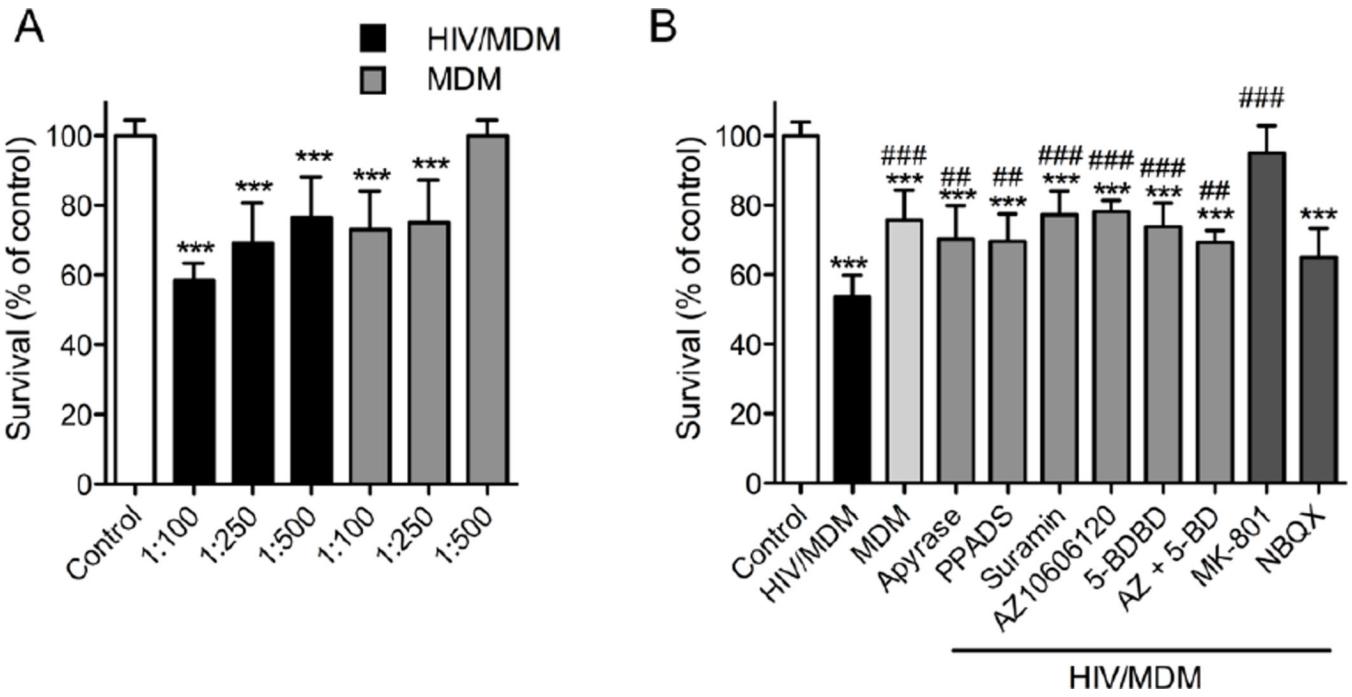

Figure 4. Calcium permeable purinergic receptors regulate HIV/MDM-evoked excitotoxicity

Apoptotic nuclei with condensed or fragmented chromatin were determined by Hoechst 33342 DNA staining in neurons exposed to high-dose MDM or HIV/MDM supernatants (1:100 dilution) for 24 h. **(A)** Dose–dependent effect on neuronal survival upon exposure to MDM or HIV/MDM supernatants. **(B)** Neuronal apoptosis induced by HIV/MDM supernatants (1:100) was reduced by pre-treatment of HIV/MDM supernatant with apyrase (2 IU/10 μl HIV/MDM), and general antagonists of purinergic receptors (PPADS; 10 μM and Suramin; 100 μM), specific antagonists of $P2X_7$ (AZ10606120; 10 μM), $P2X_4$ (5-BDBD; 10 μM) and AMPA receptors (NBQX; 10 μM). Neuronal death was completely blocked by an antagonist to NMDA receptors (MK-801; 10 μM). Data are the average ± S.D. of 200 cells from three separate experiments per condition. ANOVA with Tukey's post hoc comparisons. *** = $p < 0.001$, ** = $p < 0.01$ compared with control, and ### = $p < 0.001$, ## = $p < 0.01$ compared with HIV/MDM supernatant.

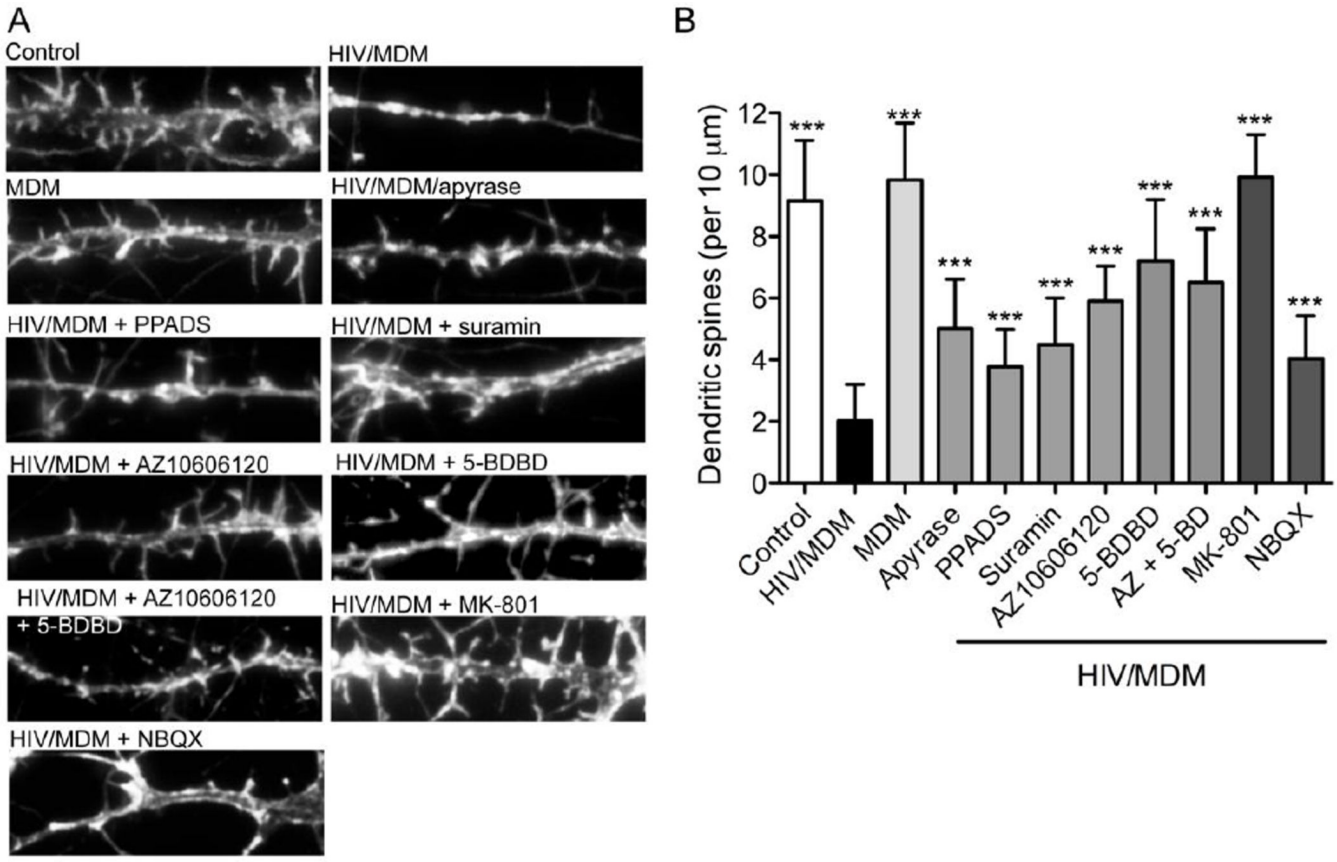

Figure 5. Purinergic and NMDA receptors mediate the downregulation of dendritic spines in response to low dose HIV/MDM supernatants

Neuronal dendrites were visualized by labeling F-actin with fluorescent phalloidin. **(A)** Representative images showing individual dendritic branches and associated spines in neurons treated with vehicle (Control), low dose HIV/MDM supernatants (1:250), MDM supernatants (1:250), and HIV/MDM supernatants in the presence of apyrase (2 IU/10 μl), or antagonists of purinergic receptors (PPADS; 10 μM and suramin; 100 μM), $P2X_7$ (AZ10606120; 10 μM), $P2X_4$ (5-BDBD; 10 μM), NMDA (MK801; 10 μM), and AMPA (NBQX; 10 μM). **(B)** Quantitative analysis of dendritic spine numbers. HIV/MDM supernatant-induced downregulation of dendritic spines was attenuated by degradation of ATP, purinergic, and AMPA receptor antagonists. NMDA-receptor blockade provided near complete protection from HIV/MDM induced downregulation of dendritic spine number. Quantitative data are the average ± S.D. of dendritic spine number per 10 μm. Data were obtained from a total of 10 different neurons in 3 independent experiments per condition. ANOVA with Tukey's post hoc comparisons. *** = $p < 0.001$ compared with HIV/MDM sup.

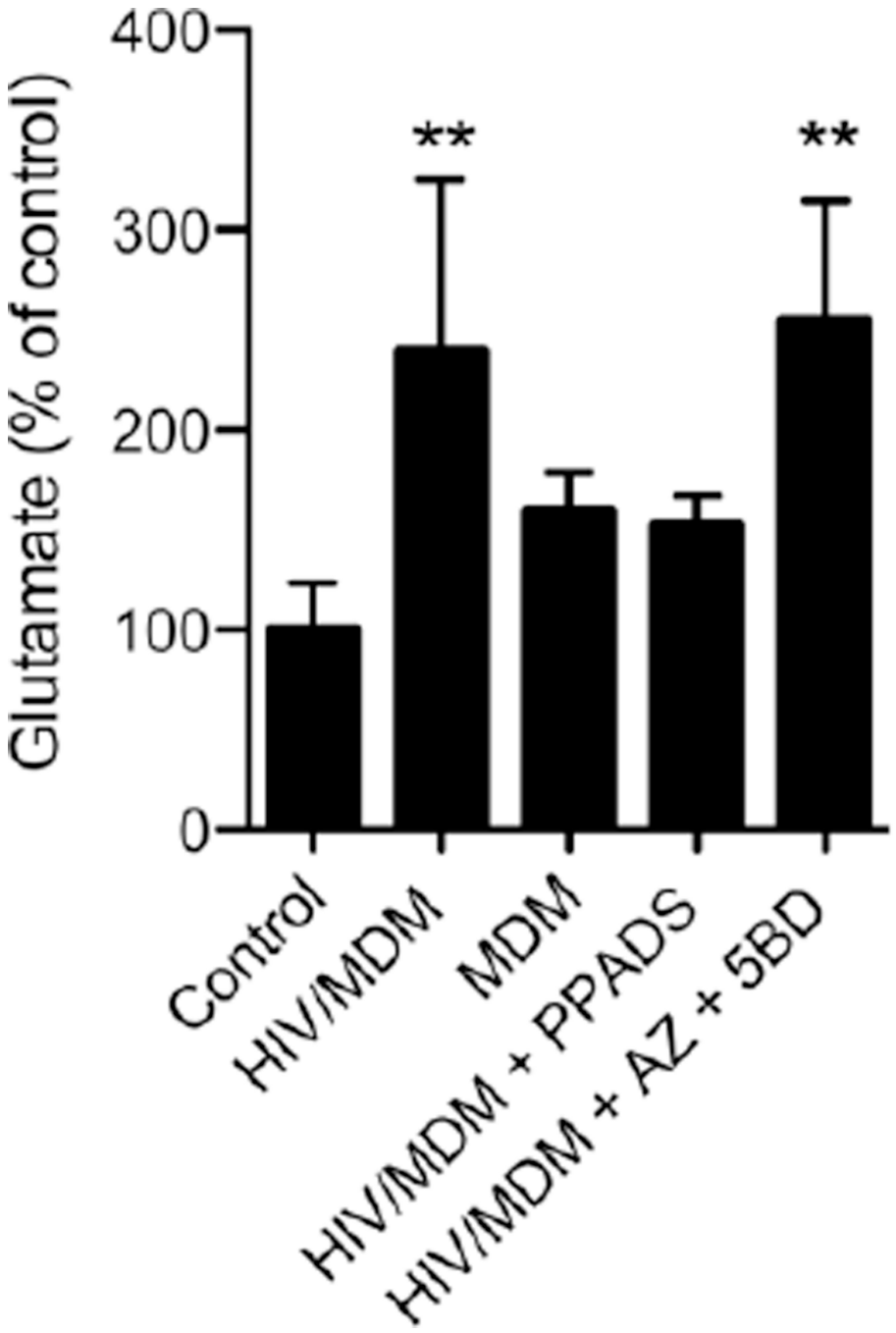

Figure 6. ATP contained in HIV/MDM supernatants increases extracellular glutamate by a purinergic receptor mediated mechanism

Hippocampal neuronal cultures were subjected to 5 min incubations with HIV/MDM (1:100) in the presence of DL-TBOA (70 μM) to block glutamate transporters. HIV/MDM supernatants induced a 2.5-fold increase in the content of extracellular glutamate that was blocked by PPADS (10 μM), but not by co-administration of antagonists for P2×4 and $P2X_7$ receptors (5-BDBD (5BD) + AZ10606120 (AZ); 10 μM each). Experiments were conducted in quadruplicate. Values are mean ± S.D. of glutamate normalized to controls. ANOVA with Tukey's post hoc comparisons ** = $p < 0.01$ compared to control.

Table 1

ATP concentrations in supernatants from HIV infected MDM (HIV/MDM) and mock-infected MDM (individual blood donors are indicated as d1-d3).

	Adenosine (μM)	**AMP (μM)**	**ADP (μM)**	**ATP (μM)**
HIV/MDM-d1	0.01	31.7	16.8	70.5
HIV/MDM-d2	ND	17.3	16.3	67.4
HIV/MDM-d3	ND	32.2	22.2	66.9
Mock-MDS	0.16	4.5	4.1	13.7